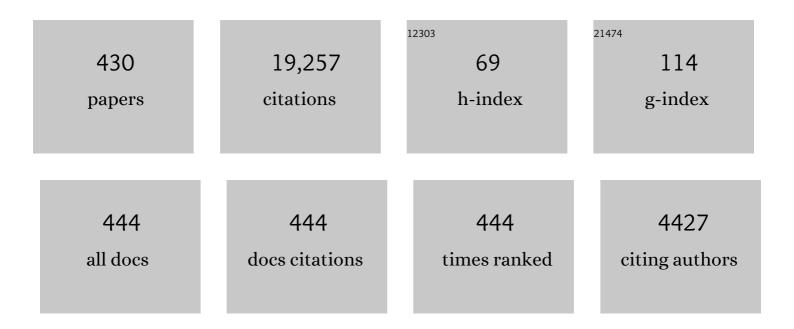
List of Publications by Year in descending order

Source: https://exaly.com/author-pdf/3605283/publications.pdf Version: 2024-02-01



H E SDENCE

#	Article	IF	CITATIONS
1	Rapid local acceleration of relativistic radiation-belt electrons by magnetospheric chorus. Nature, 2013, 504, 411-414.	13.7	608
2	The Magnetic Electron Ion Spectrometer (MagEIS) Instruments Aboard the Radiation Belt Storm Probes (RBSP) Spacecraft. Space Science Reviews, 2013, 179, 383-421.	3.7	491
3	Electron Acceleration in the Heart of the Van Allen Radiation Belts. Science, 2013, 341, 991-994.	6.0	463
4	Science Goals and Overview of the Radiation Belt Storm Probes (RBSP) Energetic Particle, Composition, and Thermal Plasma (ECT) Suite on NASA's Van Allen Probes Mission. Space Science Reviews, 2013, 179, 311-336.	3.7	463
5	Helium, Oxygen, Proton, and Electron (HOPE) Mass Spectrometer for the Radiation Belt Storm Probes Mission. Space Science Reviews, 2013, 179, 423-484.	3.7	459
6	The Relativistic Electron-Proton Telescope (REPT) Instrument on Board the Radiation Belt Storm Probes (RBSP) Spacecraft: Characterization of Earth's Radiation Belt High-Energy Particle Populations. Space Science Reviews, 2013, 179, 337-381.	3.7	334
7	Lunar Reconnaissance Orbiter Overview: TheÂInstrument Suite and Mission. Space Science Reviews, 2007, 129, 391-419.	3.7	322
8	Effect of EMIC waves on relativistic and ultrarelativistic electron populations: Groundâ€based and Van Allen Probes observations. Geophysical Research Letters, 2014, 41, 1375-1381.	1.5	294
9	ULF waves in the solar wind as direct drivers of magnetospheric pulsations. Geophysical Research Letters, 2002, 29, 39-1-39-4.	1.5	256
10	A Long-Lived Relativistic Electron Storage Ring Embedded in Earth's Outer Van Allen Belt. Science, 2013, 340, 186-190.	6.0	216
11	Source and seed populations for relativistic electrons: Their roles in radiation belt changes. Journal of Geophysical Research: Space Physics, 2015, 120, 7240-7254.	0.8	215
12	Observations of discrete, global magnetospheric oscillations directly driven by solar wind density variations. Journal of Geophysical Research, 2003, 108, .	3.3	213
13	The occurrence and wave properties of H ⁺ â€, He ⁺ â€, and O ⁺ â€band EMIC waves observed by the Van Allen Probes. Journal of Geophysical Research: Space Physics, 2015, 120, 7477-7492.	0.8	184
14	Radiation belt electron acceleration by chorus waves during the 17 March 2013 storm. Journal of Geophysical Research: Space Physics, 2014, 119, 4681-4693.	0.8	182
15	Characteristics of ion flow in the quiet state of the inner plasma sheet. Geophysical Research Letters, 1993, 20, 1711-1714.	1.5	177
16	Energyâ€dependent dynamics of keV to MeV electrons in the inner zone, outer zone, and slot regions. Journal of Geophysical Research: Space Physics, 2016, 121, 397-412.	0.8	152
17	CEPPAD. Space Science Reviews, 1995, 71, 531-562.	3.7	150
18	Evolution and slow decay of an unusual narrow ring of relativistic electrons near L ~ 3.2 following the September 2012 magnetic storm. Geophysical Research Letters, 2013, 40, 3507-3511.	1.5	150

#	Article	IF	CITATIONS
19	Wave-driven butterfly distribution of Van Allen belt relativistic electrons. Nature Communications, 2015, 6, 8590.	5.8	148
20	Coronal mass ejections, magnetic clouds, and relativistic magnetospheric electron events: ISTP. Journal of Geophysical Research, 1998, 103, 17279-17291.	3.3	144
21	Cusp energetic particle events: Implications for a major acceleration region of the magnetosphere. Journal of Geophysical Research, 1998, 103, 69-78.	3.3	143
22	Magnetospheric plasma pressures in the midnight meridian: Observations from 2.5 to 35 R _E . Journal of Geophysical Research, 1989, 94, 5264-5272.	3.3	137
23	Eventâ€specific chorus wave and electron seed population models in DREAM3D using the Van Allen Probes. Geophysical Research Letters, 2014, 41, 1359-1366.	1.5	136
24	A statistical study of EMIC waves observed by Cluster: 1. Wave properties. Journal of Geophysical Research: Space Physics, 2015, 120, 5574-5592.	0.8	136
25	Excitation of poloidal standing Alfvén waves through drift resonance waveâ€particle interaction. Geophysical Research Letters, 2013, 40, 4127-4132.	1.5	134
26	The average magnetic field draping and consistent plasma properties of the Venus magnetotail. Journal of Geophysical Research, 1986, 91, 7939-7953.	3.3	133
27	Recurrent geomagnetic storms and relativistic electron enhancements in the outer magnetosphere: ISTP coordinated measurements. Journal of Geophysical Research, 1997, 102, 14141-14148.	3.3	133
28	Interstellar Mapping and Acceleration Probe (IMAP): A New NASA Mission. Space Science Reviews, 2018, 214, 1.	3.7	129
29	Van Allen Probes observation of localized drift resonance between poloidal mode ultra″ow frequency waves and 60 keV electrons. Geophysical Research Letters, 2013, 40, 4491-4497.	1.5	127
30	Gradual diffusion and punctuated phase space density enhancements of highly relativistic electrons: Van Allen Probes observations. Geophysical Research Letters, 2014, 41, 1351-1358.	1.5	127
31	Van Allen probes, NOAA, GOES, and ground observations of an intense EMIC wave event extending over 12 h in magnetic local time. Journal of Geophysical Research: Space Physics, 2015, 120, 5465-5488.	0.8	127
32	Wave-induced loss of ultra-relativistic electrons in the Van Allen radiation belts. Nature Communications, 2016, 7, 12883.	5.8	127
33	CRaTER: The Cosmic Ray Telescope for the Effects ofÂRadiation Experiment on the Lunar Reconnaissance Orbiter Mission. Space Science Reviews, 2010, 150, 243-284.	3.7	123
34	An unusual enhancement of lowâ€frequency plasmaspheric hiss in the outer plasmasphere associated with substormâ€injected electrons. Geophysical Research Letters, 2013, 40, 3798-3803.	1.5	120
35	The Energetic Particle Detector (EPD) Investigation and the Energetic Ion Spectrometer (EIS) for the Magnetospheric Multiscale (MMS) Mission. Space Science Reviews, 2016, 199, 471-514.	3.7	111
36	On the cause and extent of outer radiation belt losses during the 30 September 2012 dropout event. Journal of Geophysical Research: Space Physics, 2014, 119, 1530-1540.	0.8	110

#	Article	IF	CITATIONS
37	Resonant scattering of energetic electrons by unusual low-frequency hiss. Geophysical Research Letters, 2014, 41, 1854-1861.	1.5	110
38	Van Allen Probes show that the inner radiation zone contains no MeV electrons: ECT/MagEIS data. Geophysical Research Letters, 2015, 42, 1283-1289.	1.5	109
39	Heliospheric plasma sheets. Journal of Geophysical Research, 2004, 109, .	3.3	107
40	Quantifying the radiation belt seed population in the 17 March 2013 electron acceleration event. Geophysical Research Letters, 2014, 41, 2275-2281.	1.5	107
41	Metrics for solar wind prediction models: Comparison of empirical, hybrid, and physicsâ€based schemes with 8 years of L1 observations. Space Weather, 2008, 6, .	1.3	105
42	Discovery of the action of a geophysical synchrotron in the Earth's Van Allen radiation belts. Nature Communications, 2013, 4, .	5.8	104
43	Shockâ€induced prompt relativistic electron acceleration in the inner magnetosphere. Journal of Geophysical Research: Space Physics, 2015, 120, 1661-1674.	0.8	104
44	Competing source and loss mechanisms due to waveâ€particle interactions in Earth's outer radiation belt during the 30 September to 3 October 2012 geomagnetic storm. Journal of Geophysical Research: Space Physics, 2014, 119, 1960-1979.	0.8	103
45	First energetic neutral atom images from Polar. Geophysical Research Letters, 1997, 24, 1167-1170.	1.5	101
46	Chorus acceleration of radiation belt relativistic electrons during March 2013 geomagnetic storm. Journal of Geophysical Research: Space Physics, 2014, 119, 3325-3332.	0.8	101
47	On the possibility of quasiâ€static convection in the quiet magnetotail. Geophysical Research Letters, 1988, 15, 1541-1544.	1.5	98
48	Explaining the dynamics of the ultra-relativistic third Van Allen radiation belt. Nature Physics, 2016, 12, 978-983.	6.5	97
49	The global response of relativistic radiation belt electrons to the January 1997 magnetic cloud. Geophysical Research Letters, 1998, 25, 3265-3268.	1.5	96
50	Observations Directly Linking Relativistic Electron Microbursts to Whistler Mode Chorus: Van Allen Probes and FIREBIRD II. Geophysical Research Letters, 2017, 44, 11,265.	1.5	96
51	Simulation of Van Allen Probes plasmapause encounters. Journal of Geophysical Research: Space Physics, 2014, 119, 7464-7484.	0.8	95
52	Contributions of the lowâ€latitude boundary layer to the finite width magnetotail convection model. Journal of Geophysical Research, 1993, 98, 15487-15496.	3.3	94
53	Highly relativistic radiation belt electron acceleration, transport, and loss: Large solar storm events of March and June 2015. Journal of Geophysical Research: Space Physics, 2016, 121, 6647-6660.	0.8	93
54	Unraveling the drivers of the storm time radiation belt response. Geophysical Research Letters, 2015, 42, 3076-3084.	1.5	90

#	Article	IF	CITATIONS
55	AMPTE/CCE-SCATHA simultaneous observations of substorm-associated magnetic fluctuations. Journal of Geophysical Research, 1998, 103, 4671-4682.	3.3	89
56	The Fly's Eye Energetic Particle Spectrometer (FEEPS) Sensors for the Magnetospheric Multiscale (MMS) Mission. Space Science Reviews, 2016, 199, 309-329.	3.7	89
57	Prompt energization of relativistic and highly relativistic electrons during a substorm interval: Van Allen Probes observations. Geophysical Research Letters, 2014, 41, 20-25.	1.5	88
58	Formation of energetic electron butterfly distributions by magnetosonic waves via Landau resonance. Geophysical Research Letters, 2016, 43, 3009-3016.	1.5	88
59	Modeling inward diffusion and slow decay of energetic electrons in the Earth's outer radiation belt. Geophysical Research Letters, 2015, 42, 987-995.	1.5	87
60	A new, temporarily confined population in the polar cap during the August 27, 1996 geomagnetic field distortion period. Geophysical Research Letters, 1997, 24, 1447-1450.	1.5	86
61	An event-based approach to validating solar wind speed predictions: High-speed enhancements in the Wang-Sheeley-Arge model. Journal of Geophysical Research, 2005, 110, .	3.3	86
62	Quantitative Evaluation of Radial Diffusion and Local Acceleration Processes During GEM Challenge Events. Journal of Geophysical Research: Space Physics, 2018, 123, 1938-1952.	0.8	86
63	The discovery of trapped energetic electrons in the outer cusp. Geophysical Research Letters, 1998, 25, 1825-1828.	1.5	85
64	The Response of Earth's Electron Radiation Belts to Geomagnetic Storms: Statistics From the Van Allen Probes Era Including Effects From Different Storm Drivers. Journal of Geophysical Research: Space Physics, 2019, 124, 1013-1034.	0.8	84
65	Relative occurrence rates and connection of discrete frequency oscillations in the solar wind density and dayside magnetosphere. Journal of Geophysical Research, 2009, 114, .	3.3	82
66	Investigation of EMIC wave scattering as the cause for the BARREL 17 January 2013 relativistic electron precipitation event: A quantitative comparison of simulation with observations. Geophysical Research Letters, 2014, 41, 8722-8729.	1.5	78
67	A background correction algorithm for Van Allen Probes MagEIS electron flux measurements. Journal of Geophysical Research: Space Physics, 2015, 120, 5703-5727.	0.8	78
68	Radiation belt electron acceleration during the 17 March 2015 geomagnetic storm: Observations and simulations. Journal of Geophysical Research: Space Physics, 2016, 121, 5520-5536.	0.8	77
69	The dependence on geomagnetic conditions and solar wind dynamic pressure of the spatial distributions of EMIC waves observed by the Van Allen Probes. Journal of Geophysical Research: Space Physics, 2016, 121, 4362-4377.	0.8	76
70	Unraveling the excitation mechanisms of highly oblique lower band chorus waves. Geophysical Research Letters, 2016, 43, 8867-8875.	1.5	75
71	Ultra-low-frequency wave-driven diffusion of radiation belt relativistic electrons. Nature Communications, 2015, 6, 10096.	5.8	71
72	What Causes Radiation Belt Enhancements: A Survey of the Van Allen Probes Era. Geophysical Research Letters, 2018, 45, 5253-5259.	1.5	71

#	Article	IF	CITATIONS
73	The evolution of ring current ion energy density and energy content during geomagnetic storms based on Van Allen Probes measurements. Journal of Geophysical Research: Space Physics, 2015, 120, 7493-7511.	0.8	70
74	The global pattern of evolution of plasmaspheric drainage plumes. Geophysical Monograph Series, 2005, , 1-22.	0.1	69
75	Prompt acceleration of magnetospheric electrons to ultrarelativistic energies by the 17 March 2015 interplanetary shock. Journal of Geophysical Research: Space Physics, 2016, 121, 7622-7635.	0.8	68
76	Lunar radiation environment and space weathering from the Cosmic Ray Telescope for the Effects of Radiation (CRaTER). Journal of Geophysical Research, 2012, 117, .	3.3	67
77	Combined convective and diffusive simulations: VERBâ€4D comparison with 17 March 2013 Van Allen Probes observations. Geophysical Research Letters, 2015, 42, 9600-9608.	1.5	67
78	Energetic, relativistic, and ultrarelativistic electrons: Comparison of longâ€ŧerm VERB code simulations with Van Allen Probes measurements. Journal of Geophysical Research: Space Physics, 2015, 120, 3574-3587.	0.8	67
79	Direct evidence for EMIC wave scattering of relativistic electrons in space. Journal of Geophysical Research: Space Physics, 2016, 121, 6620-6631.	0.8	67
80	First multipoint in situ observations of electron microbursts: Initial results from the NSF FIREBIRD II mission. Journal of Geophysical Research: Space Physics, 2016, 121, 5272-5283.	0.8	67
81	lon observations from geosynchronous orbit as a proxy for ion cyclotron wave growth during storm times. Journal of Geophysical Research, 2009, 114, .	3.3	66
82	Dipolarizing flux bundles in the cisâ€geosynchronous magnetosphere: Relationship between electric fields and energetic particle injections. Journal of Geophysical Research: Space Physics, 2016, 121, 1362-1376.	0.8	66
83	The Global Statistical Response of the Outer Radiation Belt During Geomagnetic Storms. Geophysical Research Letters, 2018, 45, 3783-3792.	1.5	66
84	First results from CSSWE CubeSat: Characteristics of relativistic electrons in the nearâ€Earth environment during the October 2012 magnetic storms. Journal of Geophysical Research: Space Physics, 2013, 118, 6489-6499.	0.8	65
85	The source of O ⁺ in the storm time ring current. Journal of Geophysical Research: Space Physics, 2016, 121, 5333-5349.	0.8	63
86	A statistical study of the global structure of the ring current. Journal of Geophysical Research, 2004, 109, .	3.3	62
87	Solar proton events for 450 years: The Carrington event in perspective. Advances in Space Research, 2006, 38, 232-238.	1.2	62
88	Earth-Moon-Mars Radiation Environment Module framework. Space Weather, 2010, 8, n/a-n/a.	1.3	62
89	Nearâ€Earth injection of MeV electrons associated with intense dipolarization electric fields: Van Allen Probes observations. Geophysical Research Letters, 2015, 42, 6170-6179.	1.5	62
90	Nonstorm time dynamics of electron radiation belts observed by the Van Allen Probes. Geophysical Research Letters, 2014, 41, 229-235.	1.5	60

#	Article	IF	CITATIONS
91	Interactions of energetic electrons with ULF waves triggered by interplanetary shock: Van Allen Probes observations in the magnetotail. Journal of Geophysical Research: Space Physics, 2014, 119, 8262-8273.	0.8	57
92	ULF waves in the low″atitude boundary layer and their relationship to magnetospheric pulsations: A multisatellite observation. Journal of Geophysical Research, 1991, 96, 9503-9519.	3.3	56
93	Examining Periodic Solar-Wind Density Structures Observed in the SECCHI Heliospheric Imagers. Solar Physics, 2010, 267, 175-202.	1.0	56
94	Generation of unusually low frequency plasmaspheric hiss. Geophysical Research Letters, 2014, 41, 5702-5709.	1.5	56
95	Does the worsening galactic cosmic radiation environment observed by CRaTER preclude future manned deep space exploration?. Space Weather, 2014, 12, 622-632.	1.3	55
96	Excitation of EMIC waves detected by the Van Allen Probes on 28 April 2013. Geophysical Research Letters, 2014, 41, 4101-4108.	1.5	55
97	PARTICLE ACCELERATION AT LOW CORONAL COMPRESSION REGIONS AND SHOCKS. Astrophysical Journal, 2015, 810, 97.	1.6	55
98	Characteristic energy range of electron scattering due to plasmaspheric hiss. Journal of Geophysical Research: Space Physics, 2016, 121, 11,737.	0.8	54
99	Empirical modeling of the quiet time nightside magnetosphere. Journal of Geophysical Research, 1994, 99, 151.	3.3	53
100	Global energetic neutral atom (ENA) measurements and their association with theDstindex. Geophysical Research Letters, 1997, 24, 3173-3176.	1.5	53
101	Cusp energetic ions: A bow shock source. Geophysical Research Letters, 1998, 25, 3729-3732.	1.5	53
102	Relative timing of substorm onset phenomena. Journal of Geophysical Research, 2004, 109, .	3.3	53
103	Relativistic electron dynamics produced by azimuthally localized poloidal mode ULF waves: Boomerangâ€shaped pitch angle evolutions. Geophysical Research Letters, 2017, 44, 7618-7627.	1.5	53
104	Ring current electron dynamics during geomagnetic storms based on the Van Allen Probes measurements. Journal of Geophysical Research: Space Physics, 2016, 121, 3333-3346.	0.8	52
105	Origin of two-band chorus in the radiation belt of Earth. Nature Communications, 2019, 10, 4672.	5.8	52
106	The trapping of equatorial magnetosonic waves in the Earth's outer plasmasphere. Geophysical Research Letters, 2014, 41, 6307-6313.	1.5	51
107	Statistical properties of the radiation belt seed population. Journal of Geophysical Research: Space Physics, 2016, 121, 7636-7646.	0.8	51
108	Energy limits of electron acceleration in the plasma sheet during substorms: A case study with the Magnetospheric Multiscale (MMS) mission. Geophysical Research Letters, 2016, 43, 7785-7794.	1.5	51

#	Article	IF	CITATIONS
109	Modeling radiation belt radial diffusion in ULF wave fields: 2. Estimating rates of radial diffusion using combined MHD and particle codes. Journal of Geophysical Research, 2010, 115, .	3.3	50
110	Correlated Pc4–5 ULF waves, whistlerâ€mode chorus, and pulsating aurora observed by the Van Allen Probes and groundâ€based systems. Journal of Geophysical Research: Space Physics, 2015, 120, 8749-8761.	0.8	50
111	Simulation of energyâ€dependent electron diffusion processes in the Earth's outer radiation belt. Journal of Geophysical Research: Space Physics, 2016, 121, 4217-4231.	0.8	50
112	Energetic Electron Precipitation: Multievent Analysis of Its Spatial Extent During EMIC Wave Activity. Journal of Geophysical Research: Space Physics, 2019, 124, 2466-2483.	0.8	50
113	Intense duskside lower band chorus waves observed by Van Allen Probes: Generation and potential acceleration effect on radiation belt electrons. Journal of Geophysical Research: Space Physics, 2014, 119, 4266-4273.	0.8	49
114	Nonstorm time dropout of radiation belt electron fluxes on 24 September 2013. Journal of Geophysical Research: Space Physics, 2016, 121, 6400-6416.	0.8	49
115	Solar wind conditions leading to efficient radiation belt electron acceleration: A superposed epoch analysis. Geophysical Research Letters, 2015, 42, 6906-6915.	1.5	48
116	lon Heating by Electromagnetic Ion Cyclotron Waves and Magnetosonic Waves in the Earth's Inner Magnetosphere. Geophysical Research Letters, 2019, 46, 6258-6267.	1.5	48
117	Global‣cale ULF Waves Associated With SSC Accelerate Magnetospheric Ultrarelativistic Electrons. Journal of Geophysical Research: Space Physics, 2019, 124, 1525-1538.	0.8	48
118	Roles of whistler mode waves and magnetosonic waves in changing the outer radiation belt and the slot region. Journal of Geophysical Research: Space Physics, 2017, 122, 5431-5448.	0.8	47
119	The Composition of Plasma inside Geostationary Orbit Based on Van Allen Probes Observations. Journal of Geophysical Research: Space Physics, 2018, 123, 6478-6493.	0.8	47
120	Suprathermal electron isotropy in high-beta solar wind and its role in heat flux dropouts. Geophysical Research Letters, 2003, 30, .	1.5	46
121	Extreme geomagnetic disturbances due to shocks within CMEs. Geophysical Research Letters, 2015, 42, 4694-4701.	1.5	46
122	Formation of the oxygen torus in the inner magnetosphere: Van Allen Probes observations. Journal of Geophysical Research: Space Physics, 2015, 120, 1182-1196.	0.8	46
123	Magnetospheric influence on the Moon's exosphere. Journal of Geophysical Research, 2006, 111, .	3.3	45
124	New measurements of total ionizing dose in the lunar environment. Space Weather, 2011, 9, .	1.3	45
125	A statistical study of EMIC waves observed by Cluster: 2. Associated plasma conditions. Journal of Geophysical Research: Space Physics, 2016, 121, 6458-6479.	0.8	45
126	The variation of the plasma sheet polytropic index along the midnight meridian in a finite width magnetotail. Geophysical Research Letters, 1990, 17, 591-594.	1.5	44

#	Article	IF	CITATIONS
127	Role of coronal mass ejections in the heliospheric Hale cycle. Geophysical Research Letters, 2007, 34, .	1.5	44
128	Multiple loss processes of relativistic electrons outside the heart of outer radiation belt during a storm sudden commencement. Journal of Geophysical Research: Space Physics, 2015, 120, 10,275.	0.8	44
129	Update on the Worsening Particle Radiation Environment Observed by CRaTER and Implications for Future Human Deepâ€Space Exploration. Space Weather, 2018, 16, 289-303.	1.3	44
130	Static magnetic field models consistent with nearly isotropic plasma pressure. Geophysical Research Letters, 1987, 14, 872-875.	1.5	43
131	Variability of the pitch angle distribution of radiation belt ultrarelativistic electrons during and following intense geomagnetic storms: Van Allen Probes observations. Journal of Geophysical Research: Space Physics, 2015, 120, 4863-4876.	0.8	43
132	A Statistical Study of EMIC Waves Associated With and Without Energetic Particle Injection From the Magnetotail. Journal of Geophysical Research: Space Physics, 2019, 124, 433-450.	0.8	43
133	Multipoint Observations of Energetic Particle Injections and Substorm Activity During a Conjunction Between Magnetospheric Multiscale (MMS) and Van Allen Probes. Journal of Geophysical Research: Space Physics, 2017, 122, 11,481.	0.8	42
134	An Empirical Model of Radiation Belt Electron Pitch Angle Distributions Based On Van Allen Probes Measurements. Journal of Geophysical Research: Space Physics, 2018, 123, 3493-3511.	0.8	41
135	The Relationship Between EMIC Wave Properties and Proton Distributions Based on Van Allen Probes Observations. Geophysical Research Letters, 2019, 46, 4070-4078.	1.5	41
136	Direct Observation of Subrelativistic Electron Precipitation Potentially Driven by EMIC Waves. Geophysical Research Letters, 2019, 46, 12711-12721.	1.5	41
137	Space Technology 5 multiâ€point measurements of nearâ€Earth magnetic fields: Initial results. Geophysical Research Letters, 2008, 35, .	1.5	40
138	Inherent lengthâ€scales of periodic solar wind number density structures. Journal of Geophysical Research, 2008, 113, .	3.3	40
139	Plasmatrough exohiss waves observed by Van Allen Probes: Evidence for leakage from plasmasphere and resonant scattering of radiation belt electrons. Geophysical Research Letters, 2015, 42, 1012-1019.	1.5	40
140	What effect do substorms have on the content of the radiation belts?. Journal of Geophysical Research: Space Physics, 2016, 121, 6292-6306.	0.8	40
141	Revisiting two-step Forbush decreases. Journal of Geophysical Research, 2011, 116, n/a-n/a.	3.3	39
142	Second harmonic poloidal waves observed by Van Allen Probes in the duskâ€midnight sector. Journal of Geophysical Research: Space Physics, 2017, 122, 3013-3039.	0.8	39
143	Storm-time configuration of the inner magnetosphere: Lyon-Fedder-Mobarry MHD code, Tsyganenko model, and GOES observations. Journal of Geophysical Research, 2006, 111, .	3.3	38
144	Study of EMIC wave excitation using direct ion measurements. Journal of Geophysical Research: Space Physics, 2015, 120, 2702-2719.	0.8	38

#	Article	IF	CITATIONS
145	Ultrarelativistic electron butterfly distributions created by parallel acceleration due to magnetosonic waves. Journal of Geophysical Research: Space Physics, 2016, 121, 3212-3222.	0.8	38
146	On the relation between radiation belt electrons and solar wind parameters/geomagnetic indices: Dependence on the first adiabatic invariant and <i>L</i> [*] . Journal of Geophysical Research: Space Physics, 2017, 122, 1624-1642.	0.8	38
147	The hidden dynamics of relativistic electrons (0.7–1.5ÂMeV) in the inner zone and slot region. Journal of Geophysical Research: Space Physics, 2017, 122, 3127-3144.	0.8	38
148	Rapid Loss of Radiation Belt Relativistic Electrons by EMIC Waves. Journal of Geophysical Research: Space Physics, 2017, 122, 9880-9897.	0.8	38
149	A quantitative assessment of empirical magnetic field models at geosynchronous orbit during magnetic storms. Journal of Geophysical Research, 2008, 113, .	3.3	37
150	REPAD: An empirical model of pitch angle distributions for energetic electrons in the Earth's outer radiation belt. Journal of Geophysical Research: Space Physics, 2014, 119, 1693-1708.	0.8	37
151	Quantifying the relative contributions of substorm injections and chorus waves to the rapid outward extension of electron radiation belt. Journal of Geophysical Research: Space Physics, 2014, 119, 10,023.	0.8	37
152	Properties of Whistler Mode Waves in Earth's Plasmasphere and Plumes. Journal of Geophysical Research: Space Physics, 2019, 124, 1035-1051.	0.8	37
153	Are periodic solar wind number density structures formed in the solar corona?. Geophysical Research Letters, 2009, 36, .	1.5	36
154	Multiple bidirectional EMIC waves observed by Cluster at middle magnetic latitudes in the dayside magnetosphere. Journal of Geophysical Research: Space Physics, 2013, 118, 6266-6278.	0.8	36
155	Quantifying hissâ€driven energetic electron precipitation: A detailed conjunction event analysis. Geophysical Research Letters, 2014, 41, 1085-1092.	1.5	36
156	EMIC waves and associated relativistic electron precipitation on 25–26 January 2013. Journal of Geophysical Research: Space Physics, 2016, 121, 11,086.	0.8	36
157	Energetic magnetosheath ions connected to the Earth's bow shock: Possible source of cusp energetic ions. Journal of Geophysical Research, 2000, 105, 5471-5488.	3.3	34
158	Simulations of inner magnetosphere dynamics with an expanded RAMâ€SCB model and comparisons with Van Allen Probes observations. Geophysical Research Letters, 2014, 41, 2687-2694.	1.5	34
159	Disappearance of plasmaspheric hiss following interplanetary shock. Geophysical Research Letters, 2015, 42, 3129-3140.	1.5	34
160	Rapid enhancement of lowâ€energy (<100 eV) ion flux in response to interplanetary shocks based on two Van Allen Probes case studies: Implications for source regions and heating mechanisms. Journal of Geophysical Research: Space Physics, 2016, 121, 6430-6443.	0.8	34
161	Oxygen Ion Dynamics in the Earth's Ring Current: Van Allen Probes Observations. Journal of Geophysical Research: Space Physics, 2019, 124, 7786-7798.	0.8	34
162	RBSPâ€ECT Combined Spinâ€Averaged Electron Flux Data Product. Journal of Geophysical Research: Space Physics, 2019, 124, 9124-9136.	0.8	34

#	Article	IF	CITATIONS
163	Predicting magnetopause crossings at geosynchronous orbit during the Halloween storms. Space Weather, 2007, 5, n/a-n/a.	1.3	33
164	Electron butterfly distribution modulation by magnetosonic waves. Geophysical Research Letters, 2016, 43, 3051-3059.	1.5	33
165	The Characteristic Pitch Angle Distributions of 1ÂeV to 600ÂkeV Protons Near the Equator Based On Van Allen Probes Observations. Journal of Geophysical Research: Space Physics, 2017, 122, 9464-9473.	0.8	33
166	Microburst Scale Size Derived From Multiple Bounces of a Microburst Simultaneously Observed With the FIREBIRDâ€II CubeSats. Geophysical Research Letters, 2018, 45, 8811-8818.	1.5	33
167	On the standing wave mode of giant pulsations. Journal of Geophysical Research, 1992, 97, 10717-10732.	3.3	32
168	Ambient solar wind's effect on ICME transit times. Geophysical Research Letters, 2008, 35, .	1.5	32
169	Van Allen Probes observations of direct waveâ€particle interactions. Geophysical Research Letters, 2014, 41, 1869-1875.	1.5	32
170	Prompt injections of highly relativistic electrons induced by interplanetary shocks: A statistical study of Van Allen Probes observations. Geophysical Research Letters, 2016, 43, 12,317.	1.5	32
171	A Revised Look at Relativistic Electrons in the Earth's Inner Radiation Zone and Slot Region. Journal of Geophysical Research: Space Physics, 2019, 124, 934-951.	0.8	32
172	Lowâ€Energy (<keV) O ⁺ Ion Outflow Directly Into the Inner Magnetosphere: Van Allen Probes Observations. Journal of Geophysical Research: Space Physics, 2019, 124, 405-419.	0.8	32
173	Galactic cosmic ray radiation hazard in the unusual extended solar minimum between solar cycles 23 and 24. Space Weather, 2010, 8, n/a-n/a.	1.3	31
174	Penetration of magnetosonic waves into the plasmasphere observed by the Van Allen Probes. Geophysical Research Letters, 2015, 42, 7287-7294.	1.5	31
175	Simultaneous disappearances of plasmaspheric hiss, exohiss, and chorus waves triggered by a sudden decrease in solar wind dynamic pressure. Geophysical Research Letters, 2017, 44, 52-61.	1.5	31
176	The Relativistic Electron-Proton Telescope (REPT) Instrument on Board the Radiation Belt Storm Probes (RBSP) Spacecraft: Characterization of Earth's Radiation Belt High-Energy Particle Populations. , 2012, , 337-381.		31
177	Revision of empirical electric field modeling in the inner magnetosphere using Cluster data. Journal of Geophysical Research: Space Physics, 2013, 118, 4119-4134.	0.8	30
178	Explaining the apparent impenetrable barrier to ultra-relativistic electrons in the outer Van Allen belt. Nature Communications, 2018, 9, 1844.	5.8	30
179	Rapid Outer Radiation Belt Flux Dropouts and Fast Acceleration During the March 2015 and 2013 Storms: The Role of Ultra‣ow Frequency Wave Transport From a Dynamic Outer Boundary. Journal of Geophysical Research: Space Physics, 2020, 125, e2019JA027179.	0.8	30
180	Bursty energetic electrons confined in flux ropes in the cusp region. Planetary and Space Science, 2003, 51, 821-830.	0.9	29

#	Article	IF	CITATIONS
181	Center for integrated space weather modeling metrics plan and initial model validation results. Journal of Atmospheric and Solar-Terrestrial Physics, 2004, 66, 1499-1507.	0.6	29
182	CORONAL ELECTRON TEMPERATURE FROM THE SOLAR WIND SCALING LAW THROUGHOUT THE SPACE AGE. Astrophysical Journal, 2011, 739, 9.	1.6	29
183	The role of convection in the buildup of the ring current pressure during the 17 March 2013 storm. Journal of Geophysical Research: Space Physics, 2017, 122, 475-492.	0.8	29
184	The Characteristic Response of Whistler Mode Waves to Interplanetary Shocks. Journal of Geophysical Research: Space Physics, 2017, 122, 10,047.	0.8	29
185	The Outer Radiation Belt Response to the Storm Time Development of Seed Electrons and Chorus Wave Activity During CME and CIR Driven Storms. Journal of Geophysical Research: Space Physics, 2018, 123, 10,139.	0.8	29
186	Understanding the Driver of Energetic Electron Precipitation Using Coordinated Multisatellite Measurements. Geophysical Research Letters, 2018, 45, 6755-6765.	1.5	29
187	The radiation environment near the lunar surface: CRaTER observations and Geant4 simulations. Space Weather, 2013, 11, 142-152.	1.3	28
188	Van Allen Probes observations of magnetic field dipolarization and its associated O ⁺ flux variations in the inner magnetosphere at <i>L</i> < 6.6. Journal of Geophysical Research: Space Physics, 2016, 121, 7572-7589.	0.8	28
189	Lowâ€Energy (<200 eV) Electron Acceleration by ULF Waves in the Plasmaspheric Boundary Layer: Van Allen Probes Observation. Journal of Geophysical Research: Space Physics, 2017, 122, 9969-9982.	0.8	28
190	Global Survey of Plasma Sheet Electron Precipitation due to Whistler Mode Chorus Waves in Earth's Magnetosphere. Geophysical Research Letters, 2020, 47, e2020GL088798.	1.5	28
191	A study of omega bands and Ps6 pulsations on the ground, at low altitude and at geostationary orbit. Journal of Geophysical Research, 1999, 104, 14705-14715.	3.3	27
192	A positive correlation between energetic electron butterfly distributions and magnetosonic waves in the radiation belt slot region. Geophysical Research Letters, 2017, 44, 3980-3990.	1.5	27
193	Opening a Window on ICME-driven GCR Modulation in the Inner Solar System. Astrophysical Journal, 2018, 856, 139.	1.6	27
194	The FIREBIRD-II CubeSat mission: Focused investigations of relativistic electron burst intensity, range, and dynamics. Review of Scientific Instruments, 2020, 91, 034503.	0.6	27
195	The Magnetic Electron Ion Spectrometer (MagEIS) Instruments Aboard the Radiation Belt Storm Probes (RBSP) Spacecraft. , 2013, , 383-421.		27
196	Relativistic Electron Model in the Outer Radiation Belt Using a Neural Network Approach. Space Weather, 2021, 19, e2021SW002808.	1.3	27
197	Charge exchange contribution to the decay of the ring current, measured by energetic neutral atoms (ENAs). Journal of Geophysical Research, 2001, 106, 1931-1937.	3.3	26
198	Roles of empirical modeling within CISM. Journal of Atmospheric and Solar-Terrestrial Physics, 2004, 66, 1481-1489.	0.6	26

#	Article	IF	CITATIONS
199	Modeling radiation belt radial diffusion in ULF wave fields: 1. Quantifying ULF wave power at geosynchronous orbit in observations and in global MHD model. Journal of Geophysical Research, 2010, 115, .	3.3	26
200	Remote observations of ion temperatures in the quiet time magnetosphere. Geophysical Research Letters, 2011, 38, n/a-n/a.	1.5	26
201	Focusing on Size and Energy Dependence of Electron Microbursts From the Van Allen Radiation Belts. Space Weather, 2012, 10, .	1.3	26
202	Relative contributions of galactic cosmic rays and lunar proton "albedo―to dose and dose rates near the Moon. Space Weather, 2013, 11, 643-650.	1.3	26
203	Dielectric breakdown weathering of the Moon's polar regolith. Journal of Geophysical Research E: Planets, 2015, 120, 210-225.	1.5	26
204	Multi-satellite simultaneous observations of magnetopause and atmospheric losses of radiation belt electrons during an intense solar wind dynamic pressure pulse. Annales Geophysicae, 2016, 34, 493-509.	0.6	26
205	Survey of radiation belt energetic electron pitch angle distributions based on the Van Allen Probes MagEIS measurements. Journal of Geophysical Research: Space Physics, 2016, 121, 1078-1090.	0.8	26
206	Observation of the 40 keV field-aligned ion beams. Geophysical Research Letters, 1998, 25, 1617-1620.	1.5	25
207	Plasmoid in the high latitude boundary/cusp region observed by Cluster. Geophysical Research Letters, 2005, 32, .	1.5	25
208	Excitation of nightside magnetosonic waves observed by Van Allen Probes. Journal of Geophysical Research: Space Physics, 2014, 119, 9125-9133.	0.8	25
209	Deep dielectric charging of regolith within the Moon's permanently shadowed regions. Journal of Geophysical Research E: Planets, 2014, 119, 1806-1821.	1.5	25
210	Nitrate ion spikes in ice cores not suitable as proxies for solar proton events. Journal of Geophysical Research D: Atmospheres, 2016, 121, 2994-3016.	1.2	25
211	Spatial scale and duration of one microburst region on 13 August 2015. Journal of Geophysical Research: Space Physics, 2017, 122, 5949-5964.	0.8	25
212	Crossâ€scale observations of the 2015 St. Patrick's day storm: THEMIS, Van Allen Probes, and TWINS. Journal of Geophysical Research: Space Physics, 2017, 122, 368-392.	0.8	25
213	Systematic Evaluation of Lowâ€Frequency Hiss and Energetic Electron Injections. Journal of Geophysical Research: Space Physics, 2017, 122, 10,263-10,274.	0.8	25
214	Very Oblique Whistler Mode Propagation in the Radiation Belts: Effects of Hot Plasma and Landau Damping. Geophysical Research Letters, 2017, 44, 12,057.	1.5	25
215	Afternoon subauroral proton precipitation resulting from ring current—plasmasphere interaction. Geophysical Monograph Series, 2005, , 85-99.	0.1	24
216	Prompt enhancement of the Earth's outer radiation belt due to substorm electron injections. Journal of Geophysical Research: Space Physics, 2016, 121, 11,826.	0.8	24

#	Article	IF	CITATIONS
217	Electron dropout echoes induced by interplanetary shock: Van Allen Probes observations. Geophysical Research Letters, 2016, 43, 5597-5605.	1.5	24
218	A multispacecraft event study of Pc5 ultralowâ€frequency waves in the magnetosphere and their external drivers. Journal of Geophysical Research: Space Physics, 2017, 122, 5132-5147.	0.8	24
219	Artificial Neural Networks for Determining Magnetospheric Conditions. , 2018, , 279-300.		24
220	On the solar wind control of cusp aurora during northward IMF. Geophysical Research Letters, 2004, 31, .	1.5	23
221	Two groups of extremely large >30MeV solar proton fluence events. Advances in Space Research, 2006, 37, 1734-1740.	1.2	23
222	Synthesis of 3â€Ð Coronalâ€Solar Wind Energetic Particle Acceleration Modules. Space Weather, 2014, 12, 323-328.	1.3	23
223	Butterfly pitch angle distribution of relativistic electrons in the outer radiation belt: Evidence of nonadiabatic scattering. Journal of Geophysical Research: Space Physics, 2015, 120, 4279-4297.	0.8	23
224	Rapid flattening of butterfly pitch angle distributions of radiation belt electrons by whistlerâ€mode chorus. Geophysical Research Letters, 2016, 43, 8339-8347.	1.5	23
225	Observations of energetic particle escape at the magnetopause: Early results from the MMS Energetic Ion Spectrometer (EIS). Geophysical Research Letters, 2016, 43, 5960-5968.	1.5	23
226	Generation of extremely low frequency chorus in Van Allen radiation belts. Journal of Geophysical Research: Space Physics, 2017, 122, 3201-3211.	0.8	23
227	The Modulation of Plasma and Waves by Background Electron Density Irregularities in the Inner Magnetosphere. Geophysical Research Letters, 2020, 47, e2020GL088855.	1.5	23
228	Energetic Electron Precipitation Observed by FIREBIRDâ€II Potentially Driven by EMIC Waves: Location, Extent, and Energy Range From a Multievent Analysis. Geophysical Research Letters, 2021, 48, e2020GL091564.	1.5	23
229	The Relativistic Electron-Proton Telescope (REPT) Investigation: Design, Operational Properties, and Science Highlights. Space Science Reviews, 2021, 217, 1.	3.7	23
230	Global Survey of Electron Precipitation due to Hiss Waves in the Earth's Plasmasphere and Plumes. Journal of Geophysical Research: Space Physics, 2021, 126, e2021JA029644.	0.8	23
231	Geotail and LFM comparisons of plasma sheet climatology: 1. Average values. Journal of Geophysical Research, 2008, 113, .	3.3	22
232	Signatures of volatiles in the lunar proton albedo. Icarus, 2016, 273, 25-35.	1.1	22
233	Earth's magnetosphere and outer radiation belt under sub-Alfvénic solar wind. Nature Communications, 2016, 7, 13001.	5.8	22
234	Ion Bernstein instability as a possible source for oxygen ion cyclotron harmonic waves. Journal of Geophysical Research: Space Physics, 2017, 122, 5449-5465.	0.8	22

#	Article	IF	CITATIONS
235	The Warm Plasma Composition in the Inner Magnetosphere During 2012–2015. Journal of Geophysical Research: Space Physics, 2017, 122, 11,018.	0.8	22
236	Van Allen Probes Measurements of Energetic Particle Deep Penetration Into the Low L Region (<i>L</i> Â<Â4) During the Storm on 8 April 2016. Journal of Geophysical Research: Space Physics, 2017, 122, 12,140.	0.8	22
237	The rate of dielectric breakdown weathering of lunar regolith in permanently shadowed regions. Icarus, 2017, 283, 352-358.	1.1	22
238	Energization of the Ring Current by Substorms. Journal of Geophysical Research: Space Physics, 2018, 123, 8131-8148.	0.8	22
239	Validation of PREDICCS using LRO/CRaTER observations during three major solar events in 2012. Space Weather, 2013, 11, 350-360.	1.3	21
240	Prediction of MeV electron fluxes throughout the outer radiation belt using multivariate autoregressive models. Space Weather, 2015, 13, 853-867.	1.3	21
241	"Trunkâ€like†heavy ion structures observed by the Van Allen Probes. Journal of Geophysical Research: Space Physics, 2015, 120, 8738-8748.	0.8	21
242	Galactic cosmic ray variations in the inner heliosphere from solar distances less than 0.5 AU: Measurements from the MESSENGER Neutron Spectrometer. Journal of Geophysical Research: Space Physics, 2016, 121, 7398-7406.	0.8	21
243	A Comparative Study of ULF Waves' Role in the Dynamics of Charged Particles in the Plasmasphere: Van Allen Probes Observation. Journal of Geophysical Research: Space Physics, 2018, 123, 5334-5343.	0.8	21
244	Cold Plasmaspheric Electrons Affected by ULF Waves in the Inner Magnetosphere: A Van Allen Probes Statistical Study. Journal of Geophysical Research: Space Physics, 2019, 124, 7954-7965.	0.8	21
245	The March 2015 Superstorm Revisited: Phase Space Density Profiles and Fast ULF Wave Diffusive Transport. Journal of Geophysical Research: Space Physics, 2019, 124, 1143-1156.	0.8	21
246	Simulation studies of ionospheric airglow signatures of plasma depletions at the equator. Journal of Atmospheric and Solar-Terrestrial Physics, 1985, 47, 885-893.	0.9	20
247	The formation of molecular hydrogen from water ice in the lunar regolith by energetic charged particles. Journal of Geophysical Research E: Planets, 2013, 118, 1257-1264.	1.5	20
248	Van Allen Probes observations linking radiation belt electrons to chorus waves during 2014 multiple storms. Journal of Geophysical Research: Space Physics, 2015, 120, 938-948.	0.8	20
249	Ion nose spectral structures observed by the Van Allen Probes. Journal of Geophysical Research: Space Physics, 2016, 121, 12,025.	0.8	20
250	The influences of solar wind pressure and interplanetary magnetic field on global magnetic field and outer radiation belt electrons. Geophysical Research Letters, 2016, 43, 7319-7327.	1.5	20
251	Transitional behavior of different energy protons based on Van Allen Probes observations. Geophysical Research Letters, 2017, 44, 625-633.	1.5	20
252	EMIC Wave Events During the Four GEM QARBM Challenge Intervals. Journal of Geophysical Research: Space Physics, 2018, 123, 6394-6423.	0.8	20

#	Article	IF	CITATIONS
253	DMSP F7 observations of a substorm fieldâ€aligned current. Journal of Geophysical Research, 1991, 96, 19409-19415.	3.3	19
254	First polar and 1995-034 observations of the midaltitude cusp during a persistent northward IMF condition. Geophysical Research Letters, 1997, 24, 1475-1478.	1.5	19
255	Solar And Cosmic Ray Physics And The Space Environment: Studies For And With LISA. AIP Conference Proceedings, 2006, , .	0.3	19
256	Posteruptive phenomena in coronal mass ejections and substorms: Indicators of a universal process?. Journal of Geophysical Research, 2008, 113, .	3.3	19
257	Measurements of galactic cosmic ray shielding with the CRaTER instrument. Space Weather, 2013, 11, 284-296.	1.3	19
258	Heavyâ€ i on dominance near Cluster perigees. Journal of Geophysical Research: Space Physics, 2015, 120, 10,485.	0.8	19
259	Physical mechanism causing rapid changes in ultrarelativistic electron pitch angle distributions right after a shock arrival: Evaluation of an electron dropout event. Journal of Geophysical Research: Space Physics, 2016, 121, 8300-8316.	0.8	19
260	Eastward Propagating Second Harmonic Poloidal Waves Triggered by Temporary Outward Gradient of Proton Phase Space Density: Van Allen Probe A Observation. Journal of Geophysical Research: Space Physics, 2019, 124, 9904-9923.	0.8	19
261	Predicting magnetospheric dynamics with a coupled Sunâ€ŧoâ€Earth model: Challenges and first results. Space Weather, 2007, 5, .	1.3	18
262	The deep space galactic cosmic ray lineal energy spectrum at solar minimum. Space Weather, 2013, 11, 361-368.	1.3	18
263	The relationship between the plasmapause and outer belt electrons. Journal of Geophysical Research: Space Physics, 2016, 121, 8392-8416.	0.8	18
264	Radiation belt seed population and its association with the relativistic electron dynamics: A statistical study. Journal of Geophysical Research: Space Physics, 2017, 122, 5261-5276.	0.8	18
265	The effects of magnetospheric processes on relativistic electron dynamics in the Earth's outer radiation belt. Journal of Geophysical Research: Space Physics, 2017, 122, 9952-9968.	0.8	18
266	Storm time empirical model of O ⁺ and O ⁶⁺ distributions in the magnetosphere. Journal of Geophysical Research: Space Physics, 2017, 122, 8353-8374.	0.8	18
267	Chorus Wave Modulation of Langmuir Waves in the Radiation Belts. Geophysical Research Letters, 2017, 44, 11,713.	1.5	18
268	Generation of lower and upper bands of electrostatic electron cyclotron harmonic waves in the Van Allen radiation belts. Geophysical Research Letters, 2017, 44, 5251-5258.	1.5	18
269	Particle Radiation Sources, Propagation and Interactions in Deep Space, at Earth, the Moon, Mars, and Beyond: Examples of Radiation Interactions and Effects. Space Science Reviews, 2017, 212, 1069-1106.	3.7	18
270	The Magnetic Electron Ion Spectrometer: A Review of On-Orbit Sensor Performance, Data, Operations, and Science. Space Science Reviews, 2021, 217, 80.	3.7	18

#	Article	IF	CITATIONS
271	Relativistic electron response to the combined magnetospheric impact of a coronal mass ejection overlapping with a highâ€speed stream: Van Allen Probes observations. Journal of Geophysical Research: Space Physics, 2015, 120, 7629-7641.	0.8	17
272	The complex nature of storm-time ion dynamics: Transport and local acceleration. Geophysical Research Letters, 2016, 43, 10,059-10,067.	1.5	17
273	Generation of EMIC Waves and Effects on Particle Precipitation During a Solar Wind Pressure Intensification With <i>B</i> _{<i>z</i>} >0. Journal of Geophysical Research: Space Physics, 2019, 124, 4492-4508.	0.8	17
274	Oxygen torus and its coincidence with EMIC wave in the deep inner magnetosphere: Van Allen Probe B and Arase observations. Earth, Planets and Space, 2020, 72, 111.	0.9	17
275	Surface charging analysis of high-inclination, high-altitude spacecraft: Identification and physics of the plasma source region. IEEE Transactions on Nuclear Science, 1993, 40, 1521-1524.	1.2	16
276	Investigation of magnetopause reconnection models using two colocated, low-altitude satellites: A unifying reconnection geometry. Journal of Geophysical Research, 2001, 106, 29451-29466.	3.3	16
277	Sun-to-magnetosphere modeling: CISM forecast model development using linked empirical methods. Journal of Atmospheric and Solar-Terrestrial Physics, 2004, 66, 1491-1497.	0.6	16
278	Interhemispheric observations of impulsive nitrate enhancements associated with the four large ground-level solar cosmic ray events (1940–1950). Journal of Atmospheric and Solar-Terrestrial Physics, 2009, 71, 1840-1845.	0.6	16
279	Nitrate deposition to surface snow at Summit, Greenland, following the 9 November 2000 solar proton event. Journal of Geophysical Research D: Atmospheres, 2014, 119, 6938-6957.	1.2	16
280	Update on Radiation Dose From Galactic and Solar Protons at the Moon Using the LRO/CRaTER Microdosimeter. Space Weather, 2015, 13, 363-364.	1.3	16
281	Evolution of chorus emissions into plasmaspheric hiss observed by Van Allen Probes. Journal of Geophysical Research: Space Physics, 2016, 121, 4518-4529.	0.8	16
282	The Stormâ€Time Ring Current Response to ICMEs and CIRs Using Van Allen Probe Observations. Journal of Geophysical Research: Space Physics, 2019, 124, 9017-9039.	0.8	16
283	Temperature Dependence of Plasmaspheric Ion Composition. Journal of Geophysical Research: Space Physics, 2019, 124, 6585-6595.	0.8	16
284	Parallel Acceleration of Suprathermal Electrons Caused by Whistlerâ€Mode Hiss Waves. Geophysical Research Letters, 2019, 46, 12675-12684.	1.5	16
285	Association of energetic neutral atom bursts and magnetospheric substorms. Journal of Geophysical Research, 2000, 105, 18753-18763.	3.3	15
286	MeV magnetosheath ions energized at the bow shock. Journal of Geophysical Research, 2001, 106, 19101-19115.	3.3	15
287	Assessing access of galactic cosmic rays at Moon's orbit. Geophysical Research Letters, 2009, 36, .	1.5	15
288	Van Allen Probe observations of drift-bounce resonances with Pc 4 pulsations and wave–particle interactions in the pre-midnight inner magnetosphere. Annales Geophysicae, 2015, 33, 955-964.	0.6	15

#	Article	IF	CITATIONS
289	Multipoint spacecraft observations of long-lasting poloidal Pc4 pulsations in the dayside magnetosphere on $1\hat{a}\in$ 2 May 2014. Annales Geophysicae, 2016, 34, 985-998.	0.6	15
290	Storm time impulsive enhancements of energetic oxygen due to adiabatic acceleration of preexisting warm oxygen in the inner magnetosphere. Journal of Geophysical Research: Space Physics, 2016, 121, 7739-7752.	0.8	15
291	Van Allen Probes, THEMIS, GOES, and Cluster observations of EMIC waves, ULF pulsations, and an electron flux dropout. Journal of Geophysical Research: Space Physics, 2016, 121, 1990-2008.	0.8	15
292	Diffusive Transport of Several Hundred keV Electrons in the Earth's Slot Region. Journal of Geophysical Research: Space Physics, 2017, 122, 10,235.	0.8	15
293	MMS/FEEPS Observations of Electron Microinjections Due to Kelvinâ€Helmholtz Waves and Flux Transfer Events: A Case Study. Journal of Geophysical Research: Space Physics, 2018, 123, 5364-5378.	0.8	15
294	Rapid Enhancements of the Seed Populations in the Heart of the Earth's Outer Radiation Belt: A Multicase Study. Journal of Geophysical Research: Space Physics, 2018, 123, 4895-4907.	0.8	15
295	Energetic particle sounding of the magnetopause: A contribution by Cluster/RAPID. Journal of Geophysical Research, 2004, 109, .	3.3	14
296	Statistical analysis of MMS observations of energetic electron escape observed at/beyond the dayside magnetopause. Journal of Geophysical Research: Space Physics, 2017, 122, 9440-9463.	0.8	14
297	Space physics and policy for contemporary society. Journal of Geophysical Research: Space Physics, 2017, 122, 4430-4435.	0.8	14
298	Reply to 'The dynamics of Van Allen belts revisited'. Nature Physics, 2018, 14, 103-104.	6.5	14
299	The Storm Time Development of Source Electrons and Chorus Wave Activity During CME―and CIRâ€Driven Storms. Journal of Geophysical Research: Space Physics, 2019, 124, 6438-6452.	0.8	14
300	How dielectric breakdown may contribute to the global weathering of regolith on the moon. Icarus, 2019, 319, 785-794.	1.1	14
301	Estimating the Impacts of Radiation Belt Electrons on Atmospheric Chemistry Using FIREBIRD II and Van Allen Probes Observations. Journal of Geophysical Research D: Atmospheres, 2021, 126, e2020JD033098.	1.2	14
302	Simultaneous Pulsating Aurora and Microburst Observations With Groundâ€Based Fast Auroral Imagers and CubeSat FIREBIRDâ€II. Geophysical Research Letters, 2021, 48, e2021GL094494.	1.5	14
303	Geotail and LFM comparisons of plasma sheet climatology: 2. Flow variability. Journal of Geophysical Research, 2008, 113, .	3.3	13
304	Helium, Oxygen, Proton, and Electron (HOPE) Mass Spectrometer for the Radiation Belt Storm Probes Mission. , 2013, , 423-484.		13
305	Microinjections observed by MMS FEEPS in the dusk to midnight region. Geophysical Research Letters, 2016, 43, 6078-6086.	1.5	13
306	Plasma Anisotropies and Currents in the Nearâ€Earth Plasma Sheet and Inner Magnetosphere. Journal of Geophysical Research: Space Physics, 2018, 123, 5625-5639.	0.8	13

#	Article	IF	CITATIONS
307	Response of Different Ion Species to Local Magnetic Dipolarization Inside Geosynchronous Orbit. Journal of Geophysical Research: Space Physics, 2018, 123, 5420-5434.	0.8	13
308	Comparisons of High‣inear Energy Transfer Spectra on the ISS and in Deep Space. Space Weather, 2019, 17, 396-418.	1.3	13
309	The AEPEX mission: Imaging energetic particle precipitation in the atmosphere through its bremsstrahlung X-ray signatures. Advances in Space Research, 2020, 66, 66-82.	1.2	13
310	Long term variations of galactic cosmic radiation on board the International Space Station, on the Moon and on the surface of Mars. Journal of Space Weather and Space Climate, 0, , .	1.1	13
311	A Tale of Two Radiation Belts: The Energyâ€Dependence of Selfâ€Limiting Electron Space Radiation. Geophysical Research Letters, 2021, 48, e2021GL095779.	1.5	13
312	Solar and ionospheric plasmas in the ring current region. Geophysical Monograph Series, 2005, , 179-194.	0.1	12
313	The first cosmic ray albedo proton map of the Moon. Journal of Geophysical Research, 2012, 117, .	3.3	12
314	First joint in situ and global observations of the mediumâ€energy oxygen and hydrogen in the inner magnetosphere. Journal of Geophysical Research: Space Physics, 2015, 120, 7615-7628.	0.8	12
315	The Evolution of the Plasma Sheet Ion Composition: Storms and Recoveries. Journal of Geophysical Research: Space Physics, 2017, 122, 12,040.	0.8	12
316	Temporal Evolution of Ion Spectral Structures During a Geomagnetic Storm: Observations and Modeling. Journal of Geophysical Research: Space Physics, 2018, 123, 179-196.	0.8	12
317	Drift paths of ions composing multipleâ€nose spectral structures near the inner edge of the plasma sheet. Geophysical Research Letters, 2016, 43, 11,484.	1.5	11
318	Comparing simulated and observed EMIC wave amplitudes using in situ Van Allen Probes' measurements. Journal of Atmospheric and Solar-Terrestrial Physics, 2018, 177, 190-201.	0.6	11
319	Characteristics, Occurrence, and Decay Rates of Remnant Belts Associated With Threeâ€Belt Events in the Earth's Radiation Belts. Geophysical Research Letters, 2018, 45, 12,099.	1.5	11
320	Observations of Particle Loss due to Injectionâ€Associated Electromagnetic Ion Cyclotron Waves. Journal of Geophysical Research: Space Physics, 2021, 126, e2020JA028503.	0.8	11
321	RBSPâ€ECT Combined Pitch Angle Resolved Electron Flux Data Product. Journal of Geophysical Research: Space Physics, 2021, 126, e2020JA028637.	0.8	11
322	Polar CEPPAD/IPS energetic neutral atom (ENA) images of a substorm injection. Advances in Space Research, 2000, 25, 2407-2416.	1.2	10
323	Does the space environment affect the ecosphere?. Eos, 2011, 92, 297-298.	0.1	10
324	An empirically observed pitchâ€angle diffusion eigenmode in the Earth's electron belt near <i>L[*]</i> = 5.0. Geophysical Research Letters, 2014, 41, 251-258.	1.5	10

#	Article	IF	CITATIONS
325	Determining Plasmaspheric Density From the Upper Hybrid Resonance and From the Spacecraft Potential: How Do They Compare?. Journal of Geophysical Research: Space Physics, 2020, 125, no.	0.8	10
326	Substorm Aurorae and Their Connection to the Inner Magnetosphere Journal of Geomagnetism and Geoelectricity, 1992, 44, 1251-1260.	0.8	10
327	On the Similarity and Repeatability of Fast Radiation Belt Loss: Role of the Last Closed Drift Shell. Journal of Geophysical Research: Space Physics, 2021, 126, e2021JA029957.	0.8	10
328	Collaborative Research Activities of the Arase and Van Allen Probes. Space Science Reviews, 2022, 218, .	3.7	10
329	CRRES observations of particle flux dropout events. Advances in Space Research, 1996, 18, 217-228.	1.2	9
330	GCR access to the Moon as measured by the CRaTER instrument on LRO. Geophysical Research Letters, 2010, 37, .	1.5	9
331	Simultaneous Observations of the Westward Electrojet and the Cross-Tail Current Sheet During Substorms. Geophysical Monograph Series, 0, , 123-130.	0.1	9
332	Application and testing of the <i>L</i> [*] neural network with the selfâ€consistent magnetic field model of RAMâ€SCB. Journal of Geophysical Research: Space Physics, 2014, 119, 1683-1692.	0.8	9
333	Using proton radiation from the moon to search for diurnal variation of regolith hydrogenation. Planetary and Space Science, 2018, 162, 113-132.	0.9	9
334	Exohiss wave enhancement following substorm electron injection in the dayside magnetosphere. Earth and Planetary Physics, 2018, 2, 1-12.	0.4	9
335	Episodic Occurrence of Fieldâ€Aligned Energetic Ions on the Dayside. Geophysical Research Letters, 2020, 47, e2019GL086384.	1.5	9
336	Comparison of field-aligned currents at ionospheric and magnetospheric altitudes. Advances in Space Research, 1988, 8, 343-346.	1.2	8
337	Reply to comment on "MeV magnetosheath ions energized at the bow shock―by J. Chen, T. A. Fritz, and R. B. Sheldon. Journal of Geophysical Research, 2003, 108, .	3.3	8
338	Radiation modeling in the Earth and Mars atmospheres using LRO/CRaTER with the EMMREM Module. Space Weather, 2014, 12, 112-119.	1.3	8
339	Analysis of the potential radiation hazard of the 23 July 2012 SEP event observed by STEREO A using the EMMREM model and LRO/CRaTER. Space Weather, 2015, 13, 560-567.	1.3	8
340	On the use of drift echoes to characterize onâ€orbit sensor discrepancies. Journal of Geophysical Research: Space Physics, 2015, 120, 2076-2087.	0.8	8
341	Multisatellite observations of the magnetosphere response to changes in the solar wind and interplanetary magnetic field. Annales Geophysicae, 2018, 36, 1319-1333.	0.6	8
342	Update on Galactic Cosmic Ray Integral Flux Measurements in Lunar Orbit With CRaTER. Space Weather, 2019, 17, 1011.	1.3	8

#	Article	IF	CITATIONS
343	Science Goals and Overview of the Radiation Belt Storm Probes (RBSP) Energetic Particle, Composition, and Thermal Plasma (ECT) Suite on NASA's Van Allen Probes Mission. , 2013, , 311-336.		8
344	Pitch Angle Dependence of Electron and Ion Flux Changes During Local Magnetic Dipolarization Inside Geosynchronous Orbit. Journal of Geophysical Research: Space Physics, 2020, 125, e2019JA027543.	0.8	8
345	The what, where, when, and why of magnetospheric substorm triggers. Eos, 1996, 77, 81-86.	0.1	7
346	Cusp energetic particle events measured by POLAR spacecraft. Physics and Chemistry of the Earth, Part C: Solar, Terrestrial and Planetary Science, 1999, 24, 135-140.	0.2	7
347	Plasma sheet climatology: Geotail observations and LFM model comparisons. Journal of Atmospheric and Solar-Terrestrial Physics, 2004, 66, 1351-1360.	0.6	7
348	Toward understanding radiation belt dynamics, nuclear explosion-produced artificial belts, and active radiation belt remediation: Producing a radiation belt data assimilation model. Geophysical Monograph Series, 2005, , 221-235.	0.1	7
349	Separation of spatial and temporal structure of auroral particle precipitation. Journal of Geophysical Research, 2007, 112, .	3.3	7
350	An event study to provide validation of TING and CMIT geomagnetic middleâ€latitude electron densities at the F ₂ peak. Journal of Geophysical Research, 2008, 113, .	3.3	7
351	Multipoint, high time resolution galactic cosmic ray observations associated with two interplanetary coronal mass ejections. Journal of Geophysical Research, 2009, 114, .	3.3	7
352	The CRaTER Special Issue of <i>Space Weather</i> : Building the observational foundation to deduce biological effects of space radiation. Space Weather, 2013, 11, 47-48.	1.3	7
353	Multipoint observations of the openâ€closed field line boundary as observed by the Van Allen Probes and geostationary satellites during the 14 November 2012 geomagnetic storm. Journal of Geophysical Research: Space Physics, 2015, 120, 6596-6613.	0.8	7
354	Solar modulation of the deep space galactic cosmic ray lineal energy spectrum measured by CRaTER, 2009–2014. Space Weather, 2016, 14, 247-258.	1.3	7
355	Van Allen Probes observation of plasmaspheric hiss modulated by injected energetic electrons. Annales Geophysicae, 2018, 36, 781-791.	0.6	7
356	Driftâ€Dispersed Flux Dropouts of Energetic Electrons Observed in Earth's Middle Magnetosphere by the Magnetospheric Multiscale (MMS) Mission. Geophysical Research Letters, 2019, 46, 3069-3078.	1.5	7
357	Simultaneously Formed Wedgeâ€Like Structures of Different Ion Species Deep in the Inner Magnetosphere. Journal of Geophysical Research: Space Physics, 2020, 125, e2020JA028192.	0.8	7
358	Multiâ€Event Analysis of Plasma and Field Variations in Source of Stable Auroral Red (SAR) Arcs in Inner Magnetosphere During Nonâ€6tormâ€Time Substorms. Journal of Geophysical Research: Space Physics, 2021, 126, e2020JA029081.	0.8	7
359	Simultaneous Observation of Two Isolated Proton Auroras at Subauroral Latitudes by a Highly Sensitive Allâ€6ky Camera and Van Allen Probes. Journal of Geophysical Research: Space Physics, 2021, 126, e2020JA029078.	0.8	7
360	Multipoint Measurement of Fineâ€6tructured EMIC Waves by Arase, Van Allen Probe A and Ground Stations. Geophysical Research Letters, 2021, 48, e2021GL096488.	1.5	7

#	Article	IF	CITATIONS
361	Van Allen Probes Observations of Symmetric Stormtime Compressional ULF Waves. Journal of Geophysical Research: Space Physics, 2022, 127, .	0.8	7
362	Space-time structure of the morning aurora inferred from coincident DMSP-F6, -F8, and SÃ,ndrestrÃ,m incoherent scatter radar observations. Journal of Atmospheric and Solar-Terrestrial Physics, 1993, 55, 1729-1739.	0.9	6
363	Alfvén boundaries: Noses and zippers. Advances in Space Research, 1997, 20, 445-448.	1.2	6
364	Tail lobe and open field line region entries at mid to high latitudes. Advances in Space Research, 1997, 20, 431-435.	1.2	6
365	Earth-Moon-Mars Radiation Environment Module (EMMREM). , 2007, , .		6
366	Van Allen Probes observation and modeling of chorus excitation and propagation during weak geomagnetic activities. Journal of Geophysical Research: Space Physics, 2015, 120, 6371-6385.	0.8	6
367	Efficacy of Electric Field Models in Reproducing Observed Ring Current Ion Spectra During Two Geomagnetic Storms. Journal of Geophysical Research: Space Physics, 2019, 124, 8974-8991.	0.8	6
368	A Shortâ€lived Threeâ€Belt Structure for subâ€MeV Electrons in the Van Allen Belts: Time Scale and Energy Dependence. Journal of Geophysical Research: Space Physics, 2020, 125, e2020JA028031.	0.8	6
369	Galactic Cosmic Radiation in the Interplanetary Space Through a Modern Secular Minimum. Space Weather, 2020, 18, e2019SW002428.	1.3	6
370	CRaTER observations and permissible mission duration for human operations in deep space. Life Sciences in Space Research, 2020, 26, 149-162.	1.2	6
371	Absorbed doses from GCR and albedo particles emitted by the lunar surface. Acta Astronautica, 2020, 175, 185-189.	1.7	6
372	The Energy Spectra of Electron Microbursts Between 200ÂkeV and 1ÂMeV. Journal of Geophysical Research: Space Physics, 2021, 126, e2021JA029709.	0.8	6
373	First observations by the CEPPAD imaging proton spectrometer aboard POLAR. Advances in Space Research, 1997, 20, 933-936.	1.2	5
374	On separating space and time variations of auroral precipitation: Dual DMSP-F6 and -F8 observations. Advances in Space Research, 1997, 20, 453-456.	1.2	5
375	A new look at the pulsed reconnection model of the dayside magnetopause. Advances in Space Research, 2002, 30, 2295-2300.	1.2	5
376	Reverse convection and cusp proton aurora: Cluster, polar and image observation. Advances in Space Research, 2005, 36, 1779-1784.	1.2	5
377	Broken Power-law Distributions from Low Coronal Compression Regions or Shocks. Journal of Physics: Conference Series, 2015, 642, 012025.	0.3	5
378	Interstellar Mapping and Acceleration Probe (IMAP). Journal of Physics: Conference Series, 2016, 767, 012025.	0.3	5

#	Article	IF	CITATIONS
379	Atmospheric radiation modeling of galactic cosmic rays using LRO/CRaTER and the EMMREM model with comparisons to balloon and airline based measurements. Space Weather, 2016, 14, 659-667.	1.3	5
380	Relativistic Electron Increase During Chorus Wave Activities on the 6-8 March 2016 Geomagnetic Storm. Journal of Geophysical Research: Space Physics, 2017, 122, 11,302-11,319.	0.8	5
381	Modeling the effectiveness of shielding in the earth-moon-mars radiation environment using PREDICCS: five solar events in 2012. Journal of Space Weather and Space Climate, 2017, 7, A16.	1.1	5
382	Effects of a Realistic O ⁺ Source on Modeling the Ring Current. Journal of Geophysical Research: Space Physics, 2019, 124, 9953-9962.	0.8	5
383	Sustained Oxygen Spectral Gaps and Their Dynamic Evolution in the Inner Magnetosphere. Journal of Geophysical Research: Space Physics, 2021, 126, e2020JA029092.	0.8	5
384	Parameterizations of the linear energy transfer spectrum for the CRaTER instrument during the LRO mission. Space Weather, 2010, 8, n/a-n/a.	1.3	4
385	James Van Allen and His Namesake <scp>NASA</scp> Mission. Eos, 2013, 94, 469-470.	0.1	4
386	Magnetospheric Source Region of Auroral Fingerâ€like Structures Observed by the RBSPâ€A Satellite. Journal of Geophysical Research: Space Physics, 2018, 123, 7513-7522.	0.8	4
387	Radial Response of Outer Radiation Belt Relativistic Electrons During Enhancement Events at Geostationary Orbit. Journal of Geophysical Research: Space Physics, 2020, 125, e2019JA027660.	0.8	4
388	Multipoint Observations of Quasiperiodic Emission Intensification and Effects on Energetic Electron Precipitation. Journal of Geophysical Research: Space Physics, 2021, 126, e2020JA028484.	0.8	4
389	Composition variations of major lunar elements: Possible impacts on lunar albedo spectra. Icarus, 2021, 369, 114629.	1.1	4
390	Low Altitude Signatures of the Plasma Sheet: Model Predictions of Local Time Dependence. Journal of Geomagnetism and Geoelectricity, 1996, 48, 887-895.	0.8	4
391	Achievements and Lessons Learned From Successful Small Satellite Missions for Space Weatherâ€Oriented Research. Space Weather, 2022, 20, .	1.3	4
392	Initial POLAR MFE observation of substorm signatures in the polar magnetosphere. Geophysical Research Letters, 1997, 24, 1459-1462.	1.5	3
393	ISTP: Relativistic particle acceleration and global energy transport. Advances in Space Research, 1997, 20, 1075-1080.	1.2	3
394	Energetic neutral atom imaging with the polar ceppad/ips instrument: Initial forward modeling results. Physics and Chemistry of the Earth, Part C: Solar, Terrestrial and Planetary Science, 1999, 24, 203-208.	0.2	3
395	Magnetospheric constellation: Past, present and future. Geophysical Monograph Series, 1999, , 247-262.	0.1	3
396	Formation of the LLBL in the context of a unifying magnetopause reconnection mechanism. Geophysical Monograph Series, 2003, , 131-138.	0.1	3

#	Article	IF	CITATIONS
397	Dose spectra from energetic particles and neutrons. Space Weather, 2013, 11, 547-556.	1.3	3
398	Analysis of plasmaspheric hiss wave amplitudes inferred from lowâ€altitude POES electron data: Technique sensitivity analysis. Journal of Geophysical Research: Space Physics, 2015, 120, 3552-3563.	0.8	3
399	Interplanetary space weather effects on Lunar Reconnaissance Orbiter avalanche photodiode performance. Space Weather, 2016, 14, 343-350.	1.3	3
400	Nonlinearity in chorus waves during a geomagnetic storm on 1 November 2012. Journal of Geophysical Research: Space Physics, 2016, 121, 358-373.	0.8	3
401	Precise Detections of Solar Particle Events and a New View of the Moon. Geophysical Research Letters, 2020, 47, e2019GL085522.	1.5	3
402	Longâ€īerm Observations of Galactic Cosmic Ray LET Spectra in Lunar Orbit by LRO/CRaTER. Space Weather, 2020, 18, e2020SW002543.	1.3	3
403	Comparison of Longâ€Term Lightning Activity and Inner Radiation Belt Electron Flux Perturbations. Journal of Geophysical Research: Space Physics, 2020, 125, e2019JA027763.	0.8	3
404	The Role of the Dynamic Plasmapause in Outer Radiation Belt Electron Flux Enhancement. Geophysical Research Letters, 2020, 47, e2020GL086991.	1.5	3
405	Multipoint observations of compressional Pc5 pulsations in the dayside magnetosphere and corresponding particle signatures. Annales Geophysicae, 2020, 38, 1267-1281.	0.6	3
406	Statistical Characteristics of Energetic Electron Pitch Angle Distributions in the Van Allen Probe Era: 1. Butterfly Distributions With Flux Peaks at Preferred Pitch Angles. Journal of Geophysical Research: Space Physics, 2022, 127, .	0.8	3
407	Simultaneous Observations of EMICâ€Induced Drifting Electron Holes (EDEHs) in the Earth's Radiation Belt by the Arase Satellite, Van Allen Probes, and THEMIS. Geophysical Research Letters, 2022, 49, .	1.5	3
408	A novel metric for coronal MHD models. Journal of Geophysical Research, 2009, 114, .	3.3	2
409	Radiation environment at the Moon: Comparisons of transport code modeling and measurements from the CRaTER instrument. Space Weather, 2014, 12, 329-336.	1.3	2
410	The possible contribution of dielectric breakdown to space weathering on Phobos. Advances in Space Research, 2018, 62, 2187-2198.	1.2	2
411	Global ENA Imaging and In Situ Observations of Substorm Dipolarization on 10 August 2016. Journal of Geophysical Research: Space Physics, 2020, 125, e2019JA027733.	0.8	2
412	The effects of the location and the timing of local convection electric field enhancements in the formation of ion multiple-nose structures. Journal of Atmospheric and Solar-Terrestrial Physics, 2021, 216, 105534.	0.6	2
413	Flux Enhancements of Fieldâ€Aligned Lowâ€Energy O ⁺ Ion (FALEO) in the Inner Magnetosphere: A Possible Source of Warm Plasma Cloak and Oxygen Torus. Journal of Geophysical Research: Space Physics, 2022, 127, .	0.8	2
414	MLTâ€Dependence of Sustained Spectral Gaps of Proton and Oxygen in the Inner Magnetosphere. Journal of Geophysical Research: Space Physics, 2021, 126, .	0.8	2

#	Article	IF	CITATIONS
415	Bistatic LIDAR experiment proposed for the shuttle/tethered satellite system missions. Review of Scientific Instruments, 1985, 56, 670-673.	0.6	1
416	Geospace Environment Modeling Program flourishes. Eos, 1996, 77, 237.	0.1	1
417	Towards inner magnetosphere particle and field models. Advances in Space Research, 1997, 20, 427-430.	1.2	1
418	Observed and simulated LET spectra comparison for the CRaTER instrument on LRO. , 2012, , .		1
419	Contributions of Primary Particles to Observed LET for the CRaTER Instrument on LRO. , 2013, , .		1
420	Mars-Moons Exploration, Reconnaissance, and Landed Investigation (MERLIN). , 2016, , .		1
421	Comment on "Atmospheric ionization by highâ€fluence, hard spectrum solar proton events and their probable appearance in the ice core archive―by A. L. Melott et al Journal of Geophysical Research D: Atmospheres, 2016, 121, 12,484.	1.2	1
422	CRaTER: The Cosmic Ray Telescope for the Effects ofÂRadiation Experiment on the Lunar Reconnaissance Orbiter Mission. , 2009, , 243-284.		1
423	Evidence From Galactic Cosmic Rays That the Sun Has Likely Entered a Secular Minimum in Solar Activity. Space Weather, 2022, 20, .	1.3	1
424	Dayside open field line region boundary at high altitudes. Physics and Chemistry of the Earth, Part C: Solar, Terrestrial and Planetary Science, 1999, 24, 129-133.	0.2	0
425	Scintillator-based ring current imager for nanosatellites. , 2001, , .		0
426	Acceleration and loss driven by VLF chorus: Van Allen Probes observations and DREAM model results. , 2014, , .		0
427	Deep dielectric charging and breakdown of lunar polar regolith. Journal of Physics: Conference Series, 2015, 646, 012010.	0.3	0
428	A Multiâ€Instrument Study of a Dipolarization Event in the Inner Magnetosphere. Journal of Geophysical Research: Space Physics, 2021, 126, e2021JA029294.	0.8	0
429	The Fly's Eye Energetic Particle Spectrometer (FEEPS) Sensors for the Magnetospheric Multiscale (MMS) Mission. , 2017, , 307-327.		0
430	Particle Radiation Sources, Propagation and Interactions in Deep Space, at Earth, the Moon, Mars, and Beyond: Examples of Radiation Interactions and Effects. Space Sciences Series of ISSI, 2017, , 257-294.	0.0	0